# Structural Sizing for the Lightweight Surface Manipulation System (LSMS) Architecture

Derrick C. Seubert[1], Jacob R. Martin[1], and William R. Doggett[2]
*NASA Langley Research Center, Hampton, Virginia, 23666, USA*

**As the NASA Artemis campaign matures, the need for scalable lunar lander offloading capabilities becomes more apparent and pressing. NASA expects to send landers with payload mass capacity ranging from 100s of kg to 10,000s of kg and will require payload offloading solutions as part of the logistics chain. The Lightweight Surface Manipulation System (LSMS) is one proposed scalable solution to the gap in reusable payload offloading solutions. The LSMS is a lightweight, scalable truss-based crane capable of offloading large payload masses while consuming a small fraction of the overall lander payload mass capacity. To best utilize the capabilities enabled by the scalable LSMS architecture, project planners need to be able to easily select and size an LSMS for a mission's specific offloading needs. This paper describes three unique LSMS configurations: a one-link LSMS, a two-link LSMS, and a two-link LSMS with self-offloading capability. The fundamental governing equations to select and size the optimal LSMS for specific use cases is presented for each configuration. An LSMS sized for offloading a 7 ton, 40 kW$_e$ fission surface power reactor is presented as a design example illustrating the utility of the structural sizing approach.**

## I. Nomenclature

$A_n$ = Cross sectional area of $n^{th}$ member
$b$ = Length of spreaders
$c1$ = Compression member 1 (kingpost)
$c2$ = Compression member 2 (arm)
$c3$ = Compression member 3 (forearm)
$D_{overd}$ = Ratio of spool diameter to wire diameter
$D_{spool_n}$ = Diameter of the $n^{th}$ winch spool
$E_c$ = Modulus of compression members
$F$ = Resulting tip force
$F_n$ = Force though $n^{th}$ member
$FS_c$ = Cable factor of safety
$FS_{rod}$ = Rod factor of safety
$FS_t$ = Tube factor of safety
$h2$ = Hoist cable 2
$h3$ = Hoist cable 3
$jt1$ = Joint 1
$jt2$ = Joint 2
$jt3$ = Joint 3
$k$ = Buckling factor
$L_n$ = Length of $n^{th}$ member
$L_{c1b}$ = Length of kingpost for buckling purposes
$M_p$ = Mass of payload
$M_n$ = Mass of $n^{th}$ member
$P_{cr}$ = Critical buckling load
$R/2$ = Length of arm link or forearm link
$r_1$ = Derived external width of square tube
$r_2$ = Derived internal width of square tube
$s1$ = Member in bending
$s2a$ = Joint 2 vertical spreader
$s2b$ = Joint 2 horizontal spreader
$s3a$ = Joint 3 vertical spreader
$s3b$ = Joint 3 horizontal spreader
$t$ = Minimum tube wall thickness
$t1$ = Tension member 1
$t2a$ = Arm support rod
$t2b$ = Lift off rod 2
$t3a$ = Forearm support rod
$t3b$ = Lift off rod 3
$\eta$ = Kingpost height factor
$\sigma_c$ = Ultimate strength of cable
$\sigma_{rod}$ = Ultimate strength of rod
$\rho_c$ = Cable density
$\rho_n$ = Density of $n^{th}$ member
$\rho_{rod}$ = Rod density
$\rho_{tube}$ = Tube density

[1] Research Aerospace Engineer, Structural Mechanics and Concepts Branch, AIAA Member.
[2] Research Aerospace Engineer, Structural Mechanics and Concepts Branch, AIAA Associate Fellow.

## II. Introduction

The NASA Artemis mission campaign is enabled by key lunar surface infrastructure devices that are currently in development to support crew and robotic exploration of the lunar south pole. The Lightweight Surface Manipulation System (LSMS), shown in Fig. 1, is a robotic crane-like device architecture developed at NASA Langley Research Center to perform offloading and manipulation operations [1]. By relying on tension supported members, the LSMS architecture creates an efficient infrastructure device that packages compactly while resulting in a tool that is an order of magnitude less massive than serial manipulators with equivalent capability [2][3]. As cargo and equipment transferred to the lunar environment become more massive [4], efficient offloading systems will be critical to sustainable operations. The capability of LSMS devices significantly exceeds prior offloading capabilities, which relied on astronaut assisted and serial robotic manipulation methods. Examples of past offloading solutions include a dedicated mechanism (davit) used to offload the 210-kg Apollo Lunar Roving Vehicle (LRV) [5], and the Instrument Deployment Arm on Mars Insight, which had a maximum lift capability of 29 kg [2]. Compared to traditional offloading systems like davits or ramps, where each system is bespoke to a single payload, the LSMS is able to offload multiple units and types of units within a single mission. With self-offloading capabilities, the LSMS can also be used to offload many landers over multiple missions, saving significant amounts of payload parasitic mass over the lifetime of the system architecture. Traditional systems also have much higher percent masses of the payload capacity. Studies have shown that, in a comparison with other offloading types, the LSMS proved to be an optimal solution [3][6]. The LSMS can be designed to provide offloading capability from 10s of kg to 100,000s of kg providing NASA and partners with a scalable system for a wide variety of offloading conditions [7]. Instances of the LSMS architecture capable of offloading 35 kg (LSMS -L35 [L indicates that the number is the capability in on lunar surface]) and 1000 kg (LSMS-L1000) on the Moon have been fabricated for prototype testing in the laboratory at NASA Langley [8].

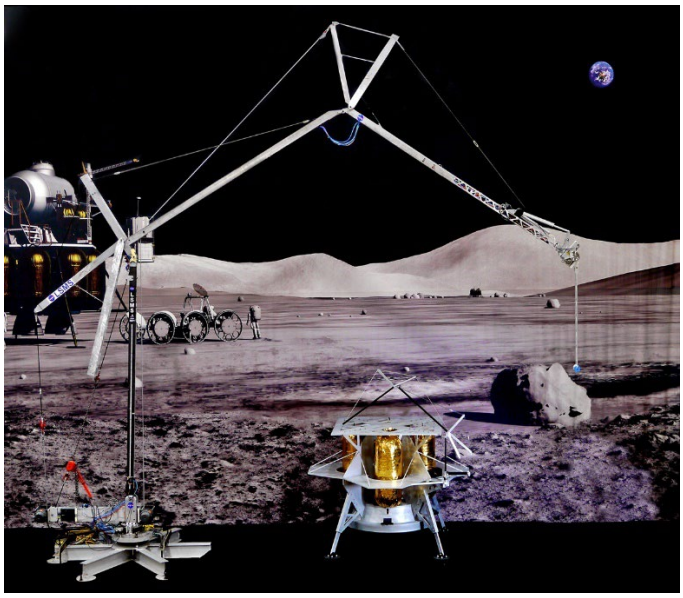


**Fig. 1 The LSMS-L1000 and LSMS-L35 shown in the laboratory at NASA Langley Research Center.**

The LSMS architecture enables an offloading device to be tailored for specific mission requirements. Mission designers need a way to size an LSMS for particular mission requirements, to estimate system and component masses, and plan architectures prior to building hardware. In this paper, a methodology to estimate overall device structural mass and structural member size given a desired device capability is provided. The designer specifies offload capability, geometric dimensions (reach, height), and degrees of freedom (DOF) for a specific mission. Then, using the analytical equations developed in this work, estimates for structural member sizes are computed. These equations enable rapid comparison and trade of different mission options. To demonstrate the comparative nature of device options, details for three architecture configurations of interest are provided, comparing both two and three degree of freedom systems. In addition, an actuation approach that enables the device to "inchworm" will be compared to a more traditional actuation arrangement. The "inch worm" maneuver is especially useful because the maneuver allows the device to self-offload, i.e., maneuver off a lander to either a mobile base or to a location in preparation for

unloading a second lander, thus negating the need to have a device on each lander when launched or present at the landing site.

The configuration of a two-link LSMS is labeled in Fig. 2 below and provides the naming convention for the structural members within the system. The two-link configuration has a total of three DOF: one for rotation at the waist (joint 1), one at the top of the kingpost that controls shoulder rotation (joint 2), and the last controlling elbow rotation (joint 3). The shoulder and elbow joints are actuated through tension cables that connect to hoists/spools located near the waist and shoulder. Spreaders at the shoulder and elbow joints allow the tension members to maintain moment arms for respective joints. Spreaders are labeled as *s#a* or *s#b* where the # is the joint number and the following letter is determined counterclockwise. Tension rods are labelled similarly to spreaders, ranging from *t#a* to *t#b*. The one-link configuration removes elements required for the elbow joint, while the self-offloading configuration can move spool 3 down to the waist and modifies the cable 3 path accordingly.

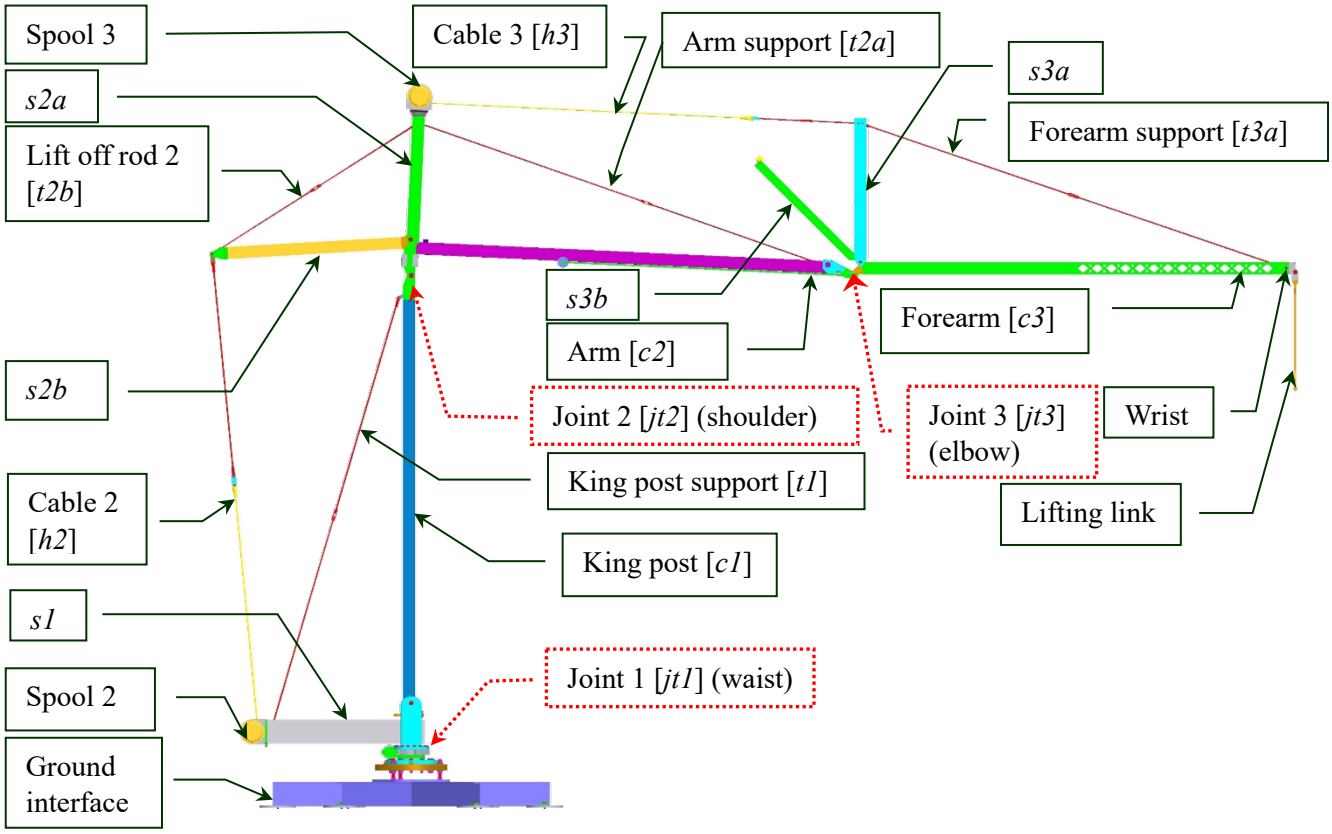



**Fig. 2 LSMS naming convention.**

## III. Square Tube LSMS Configurations

The original LSMS prototype, designed at NASA Langley in the early 2000s, uses commercial-off-the-self square aluminum tubes for compression members [1], and square-tube configurations will be assumed for the work presented herein. To properly size member lengths and thicknesses, member force equations were derived to characterize a configuration. The following sections discuss the equations for one-link, two-link, and two-link with self-offload configurations for a LSMS with tubular compression members.

### A. One-Link Equations

The one-link configuration is optimal for payload offloading operations that require minimal movement or manipulation of the payload. The one-link LSMS consists of a kingpost (*c1*) and arm (*c2*), with two spreaders (*s2a* and *s2b*) at the shoulder joint, making the one-link the simplest and lightest configuration of the set. Using the tip force, *F*, and geometric parameters shown in Fig. 3, the static forces through all members were determined symbolically using statics. Then, the length and cross-sectional area of each member is defined to determine the structural mass of the members and overall system.

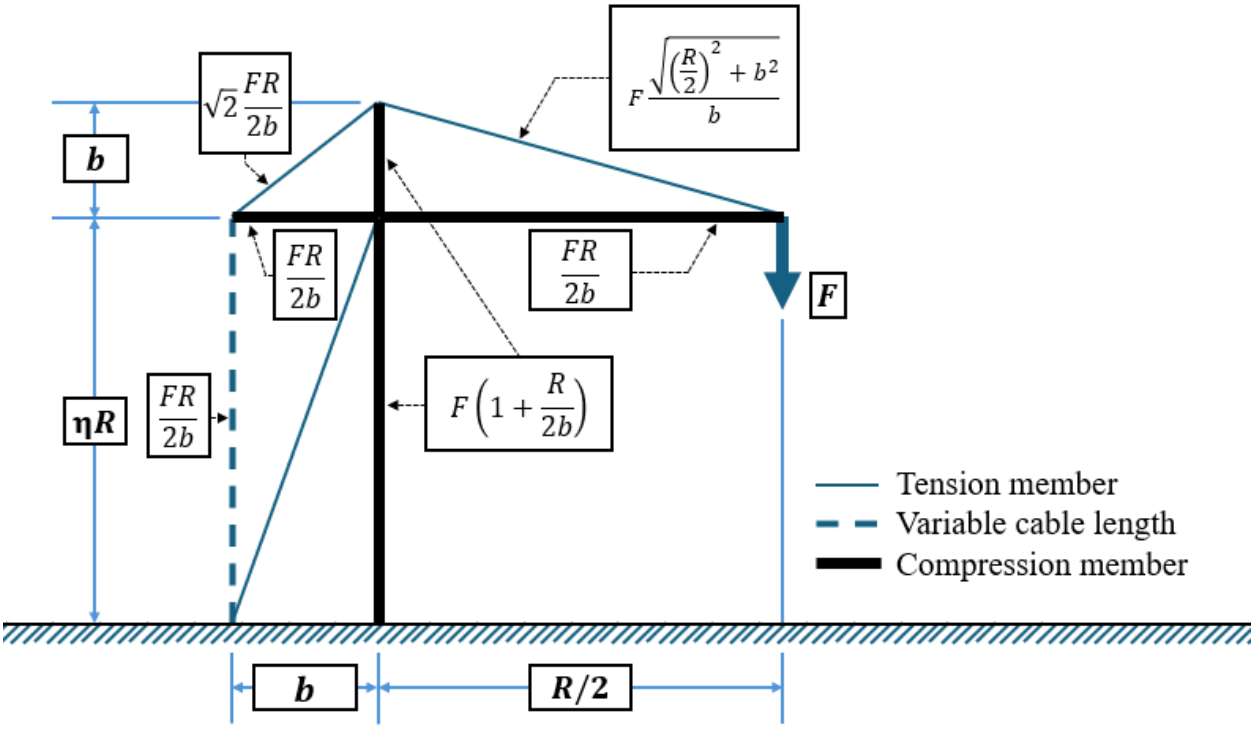



**Fig. 3 Geometry and forces of a one-link configuration.**

The force within each member of the configuration was defined in terms of the payload force ($F$) applied at the tip of the arm. The full-extension pose is chosen as it will show worst-case member loading. However, this full extension pose may not be the worst case for buckling so additional analysis may be needed for complete kingpost sizing. All spreaders are chosen to be the same length. Starting with the compression members, the arm (*c2*), along with the leftmost spreader (*s2b*) at the shoulder, experiences a force ($F_{c2}$) defined in Eq. (1) below,

$$F_{c2} = F_{s2b} = \frac{FR}{2b} \tag{1}$$

where $R$ is the reach of a two-link LSMS, $R/2$ is the reach of a single-link LSMS, and $b$ is the length of the spreaders. The compression loads in the kingpost (*c1*) and vertical spreader (*s2a*) both have the same relation to $F$, shown in Eq. (2) below.

$$F_{c1} = F_{s2a} = F\left(1+\frac{R}{2b}\right) \tag{2}$$

The force through the tension member spanning the shoulder spreaders (*t2b*) is governed by Eq. (3).

$$F_{t2b} = \sqrt{2}\frac{FR}{2b} \tag{3}$$

The force through the tension member spanning between *s2a* and joint 3 (*t2a*) is defined by Eq. (4).

$$F_{t2a} = F\frac{\sqrt{\left(\frac{R}{2}\right)^2+b^2}}{b} \tag{4}$$

Statically, for the configuration outlined Fig. 3, the tension member that keeps the kingpost vertical (*t1*) is a zero-force member. The force used in the sizing of *t1* is related to that in *t2a* by Eq. (5),

$$F_{t1} = 0.7 \cdot F_{t2a} \tag{5}$$

where the factor of 0.7 was heuristically determined and would be refined using finite element analysis as part of the design process.

The lengths ($L_n$) and cross-sectional areas ($A_n$) of each member are used with material density ($\rho_n$) to calculate the expected mass of a configuration. Following the same order as before, the lengths of each member are described below. The length of *c2* is described in Eq. (6) below.

$$L_{c2} = \frac{R}{2} \tag{6}$$

Both spreaders have equivalent lengths, shown in Eq. (7).

$$L_{s2b} = L_{s2a} = \mathrm{b} \tag{7}$$

The kingpost related to $R$ using the kingpost height factor, $\eta$, to allow for differing kingpost lengths related to arm lengths, shown below.

$$L_{c1} = (\eta \cdot R) \tag{8}$$

To more conservatively model the buckling case, the *c1* and *s2a* members were combined as a single length ($L_{c1b}$) for buckling calculations only as defined by Eq. (9).

$$L_{c1b} = (\eta \cdot R) + \mathrm{b} \tag{9}$$

The length of cable 2 (*h2*) includes the cable needed to wind around the drum spool diameter ($D_{spool_h2}$) and is defined by Eq. (10) where $A_n$ is the cross sectional area of $n^{\text{th}}$ cable and ($D_{overd}$) is the ratio of cable diameter to spool diameter. The length, $L_{h2}$, calculated in Eq. (11) uses the length of cable for two wraps around the spool in addition to the length of cable needed for LSMS in the full extension pose, while normal operations would require more cable on the spool in order for the LSMS to achieve all desired poses. The exact cable length needed will be dependent on the desired end effector poses at the end of the LSMS and should be calculated for each application before true sizing and mass estimates can be considered accurate.

$$D_{spool_n} = D_{overd} * (2\sqrt{A_n/\pi}) \tag{10}$$

$$L_{h2} = (\eta \cdot R) + \left(2 \cdot D_{spool_h2} \cdot \pi\right) \tag{11}$$

The length of *t2b* uses the Pythagorean Theorem to calculate the diagonal distance from the ends of spreaders *s2b* and *s2a*, simplified into Eq. (12).

$$L_{t2b} = \sqrt{2b^2} \tag{12}$$

The lengths of *t2a* and *t1* are similarly derived, shown in Eq. (13) and Eq. (14) below.

$$L_{t2a} = \sqrt{b^2 + \left(\frac{R}{2}\right)^2} \tag{13}$$

$$L_{t1} = \sqrt{b^2 + (\eta \cdot R)^2} \tag{14}$$

The minimum cross-sectional area, $A_n$, of members was calculated using the force found for each member, established factor of safety for each member, and the ultimate strength of the members. The minimum tension rod areas are shown in Eqs. (15), (16), and (17), while the minimum tension cable area is defined in Eq. (18) where $\sigma_{rod}$ is ultimate material strength of the rods, $\sigma_c$ is ultimate material strength of the cables, $FS_{rod}$ is factor of safety for rods, and $FS_c$ is factor of safety for cables.

$$A_{t2b} = \frac{F_{t2b} \cdot FS_{rod}}{\sigma_{rod}} \tag{15}$$

$$A_{t2a} = \frac{F_{t2a} \cdot FS_{rod}}{\sigma_{rod}} \tag{16}$$

$$A_{t1} = \frac{F_{t1} \cdot FS_{rod}}{\sigma_{rod}} \tag{17}$$

$$A_{h2} = \frac{F_{h2} \cdot FS_c}{\sigma_c} \tag{18}$$

Sizing the compression members is a bit more difficult as there are multiple factors at play such as compressive strength, buckling, tube width, and tube thickness. An equation can be derived by first considering the critical buckling load ($P_{cr}$) Eq. (19) and solving it for the area moment of inertia ($I$), which yields Eq. (20) where $E_c$ is modulus of compression members and $k$ is buckling factor. This result can then be related to the system of equations for the moment of inertia of a square tube Eq. (21) where $r_1$ is the external width of the tube and $r_2$ is internal width of the tube. Eq. (20) and Eq. (21) can then be set equivalent to each other in a system of equations as shown in Eq. (22) where $t$ is the minimum tube wall thickness. Solving this system of equations Eq. (22) for the external width of the square tube $r_1$ symbolically using Mathematica* yields Eq. (23) and $r_{1_n}$, the external width of the $n^{\text{th}}$ box tube where $FS_t$ is the factor of safety for compression member tubes.

$$P_{cr} = \frac{\pi^2 * \mathrm{E_c} * I}{FS_t (k*L)^2} \tag{19}$$

$$I = \frac{P_{cr} * FS_t * (kL)^2}{\pi^2 \mathrm{E_c}} \tag{20}$$

$$I = \frac{r_1^4 - r_2^4}{12} = \frac{r_1^4 - (r_1 - 2t)^4}{12} \tag{21}$$

$$\frac{P_{cr} * FS_t * (kL)^2}{\pi^2 \mathrm{E_c}} == \frac{r_1^4 - (r_1 - 2t)^4}{12} \tag{22}$$

$$\mathrm{r_{1_n}} = \mathrm{t} + \frac{\mathrm{E_c}(2\pi)^{2/3}\mathrm{t}^3}{\sqrt[3]{3} * \sqrt[3]{-27E_c^2 F_{St} k^2 L_n^2 F_n t^2 + \sqrt{3}\sqrt{243E_c^4 F_{St}^2 k^4 L_n^4 F_n^2 t^4 + 16E_c^6 \pi^4 t^{12}}}} - \frac{\sqrt[3]{-27E_c^2 F_{St} k^2 L_n^2 F_{c1} t^2 + \sqrt{3}\sqrt{243E_c^4 F_{St}^2 k^4 L_{c1}^4 F_{c1}^2 t^4 + 16E_c^6 \pi^4 t^{12}}}}{E_c (6\pi)^{2/3} t} \tag{23}$$

Once the derived external width of the square tube $r_1$ has been solved for each compression member the cross-sectional area of the compression members can be calculated as shown in Eqs. (24) to (27). (Note: in the above equations, the additional force exerted on the members by their own mass is not considered. A first order approximation of these values has been created but is not outlined in this paper for simplicity's sake and since they make such a minimal contribution to sizing and total system mass.)

$$A_{c1} = \mathrm{r_{1_c1}^2} - \left(r_{1_c1} - 2t\right)^2 \tag{24}$$

$$A_{c2} = \mathrm{r_{1_c2}^2} - \left(r_{1_c2} - 2t\right)^2 \tag{25}$$

$$A_{s2b} = \mathrm{r_{1_s2b}^2} - \left(r_{1_s2b} - 2t\right)^2 \tag{26}$$

$$A_{s2a} = \mathrm{r_{1_s2a}^2} - \left(r_{1_s2a} - 2t\right)^2 \tag{27}$$

The mass of each member is then calculated using the above length and area equations and respective density, $\rho$, of each member, shown in Eq. (28). Members *t2a*, *t2b*, and *t2* use rod density; while *h2* uses cable density; and *c1*, *c2*, *s2a*, and *s2b* use tube density.

$$M_n = L_n \cdot A_n \cdot \rho_n \tag{28}$$

**B. Two-Link Equations**

When additional dexterity or reach is needed in a similar packed volume, the two-link LSMS configuration adds a forearm (*c3*), elbow spreader (*s3a*), cable (*h3*), and tension rod (*t3a*) to the one-link design to accomplish just that.

* The use of trademarks or names of manufacturers in this report is for accurate reporting and does not constitute an official endorsement, either expressed or implied, of such products or manufacturers by the National Aeronautics and Space Administration.

The additional forces in new members and changes to previous forces can be seen in Fig. 4 below. The same assumptions from the one-link LSMS can be carried over to the two-link LSMS with the primary addition being that the arm and forearm are the same length ($R/2$).

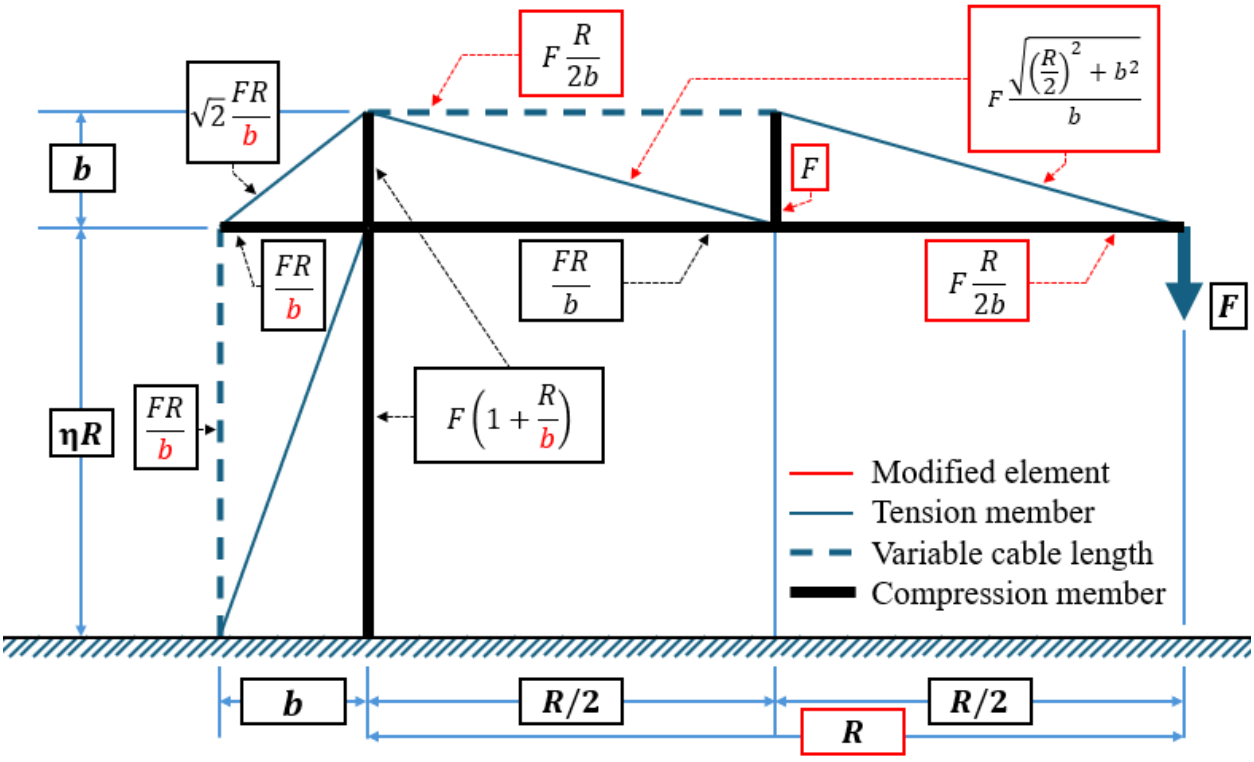



**Fig. 4 Geometry and forces for a two-link configuration.**

Forces transmitted through the cable (*h2*), upper arm (*c2*), and horizontal shoulder spreader (*s2b*) can be determined using Eq. (29) and Eq. (30), respectively:

$$F_{h2} = \frac{FR}{b} \tag{29}$$

$$F_{c2} = F_{s2b} = \frac{FR}{b} \tag{30}$$

The force equation for the kingpost (*c1*) and the vertical spreader (*s2a*) in the two-link case differs from Eq. (2) as used in the one-link case, as shown in Eq. (31).

$$F_{c1} = F_{s2a} = F \cdot \left(1 + \frac{R}{b}\right) \tag{31}$$

The tension member spanning the shoulder spreaders (*t2b*) is shown in Eq. (32) below.

$$F_{t2b} = \sqrt{2}\frac{FR}{b} \tag{32}$$

The force through tension members, *t2a* and *t3a* is defined by Eq. (33) as shown below.

$$F_{t3a} = F_{t2a} = F\frac{\sqrt{\left(\frac{R}{2}\right)^2 + b^2}}{b} \tag{33}$$

Statically, for the configuration outlined Fig. 4 and Fig. 5, the tension member that keeps the kingpost vertical (*t1*) is a zero-force member. The force used in the sizing of *t1* is related to that in *t2a* by Eq. (34), where the factor of 0.7 was heuristically determined and would be refined using finite element analysis as part of the design process.

$$F_{t1} = 0.7 \cdot F_{t2a} \tag{34}$$

The force through the vertical elbow spreader (*s3a*) is equal to the payload force, as shown in Eq. (35).

$$F_{s3a} = F \tag{35}$$

For the elbow tension members, the leftmost cable (*h3*) has the same relation as compression member *c3*, using Eq. (36).

$$F_{h3} = F_{c3} = \frac{FR}{2b} \tag{36}$$

The member lengths used in Eq. (6) through Eq. (14) to calculate member masses for the one-link example are relevant for the two-link configuration, however, adding another link adds an additional four member lengths that must be considered, shown in Eq. (37) to Eq. (40). The variable $L_{h3}$ is the length of cable needed for the minimum number of wraps around hoist 3 when LSMS is fully extended calculated according to Eq. (40). Similarly to the one-link LSMS extra length may be required for normal operation.

$$L_{c3} = \frac{R}{2} \tag{37}$$

$$L_{s3a} = b \tag{38}$$

$$L_{t3a} = \sqrt{b^2 + \left(\frac{R}{2}\right)^2} \tag{39}$$

$$L_{h3} = \left(\frac{R}{2}\right) + \left(2 \cdot D_{spool_h3} \cdot \pi\right) \tag{40}$$

The cross-sectional areas of each member are determined similarly to the one-link case and the updated lengths are used to calculate the expected mass of a two-link configuration.

$$A_{s3a} = \mathrm{r}_{1_s3a}^2 - \left(r_{1_s3a} - 2t\right)^2 \tag{41}$$

$$A_{c3} = \mathrm{r}_{1_c3}^2 - \left(r_{1_c3} - 2t\right)^2 \tag{42}$$

$$A_{t3a} = \frac{F_{t3a} \cdot FS_{rod}}{\sigma_{rod}} \tag{43}$$

$$A_{h3} = \frac{F_{h3} \cdot FS_c}{\sigma_c} \tag{44}$$

The mass Eq. (28) used in the one-link example is relevant here, but with the addition of another link there are also an additional four member masses that must be considered, $M_{c3}$, $M_{s3a}$, $M_{t3a}$, and $M_{h3}$.

### C. Two-Link with Self-Offloading Equations

When the reuse of the LSMS for multiple missions is desired, the LSMS design can be modified to allow for self-offloading from the lander to another asset like a mobile agent or a launch and landing facility foundation. The two-link with self-offloading has a modified the two-link configuration with the cable *h3* routed to spool 3 located at the shoulder joint (*jt3*). The change in geometry can be seen in Fig. 5, along with highlighted changes to member forces. Rerouting *h3* allows for the right leverage to perform "inchworm" locomotion of the LSMS when picking up the base while the tip is grasping a surface. The change in equations is discussed further below.

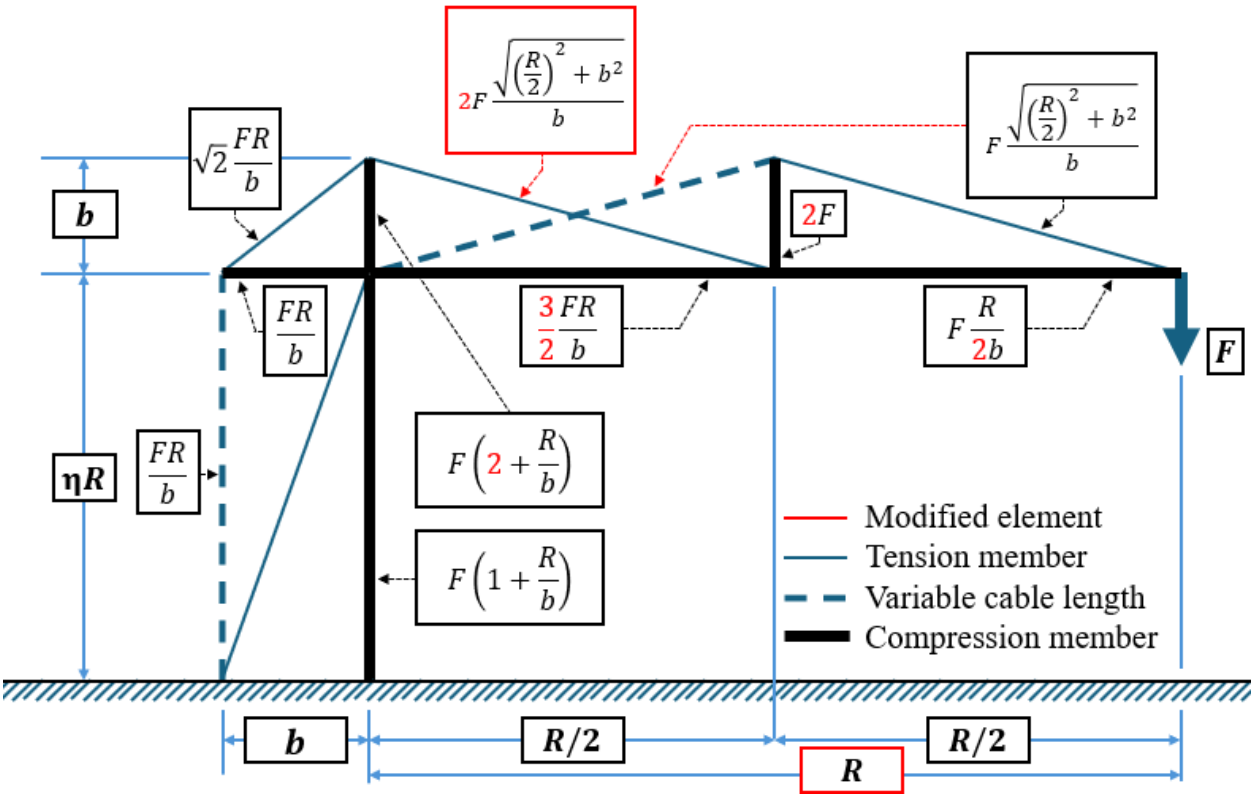



**Fig. 5 Geometry and forces for a two-link self-offload configuration.**

For the two-link self-offloading case, the same member force equations are used as in the two-link non-self-offloading case except for changes in five key member equations as highlighted in Fig. 5 and Eqs. (45) to (49).

$$F_{s2a} = F\left(\frac{R}{b}+2\right) \tag{45}$$

$$F_{t2a} = 2F \cdot \frac{\sqrt{\left(\frac{R}{2}\right)^2+b^2}}{b} \tag{46}$$

$$F_{h3} = F \cdot \frac{\sqrt{\left(\frac{R}{2}\right)^2+b^2}}{b} \tag{47}$$

$$F_{s3a} = 2F \tag{48}$$

$$F_{c2} = \frac{3FR}{2b} \tag{49}$$

The length Eqs. (6) to (14) used in the one-link example and Eqs. (37) to (40) are relevant for the two-link, self-offloading case, but with the relocation of hoist 3, $L_{h3}$ includes more cable to follow the diagonal, shown in Eq. (50).

$$L_{h3} = \sqrt{\left(\frac{R}{2}\right)^2+b^2} + \left(2 \cdot D_{spool_h3} \cdot \pi\right) \tag{50}$$

The equations for mass remain the same between the two different two-link variants. There are however a few unique considerations that must be made in order for proper kingpost sizing to occur. First, as with all variants, Eq. (9) is used as the kingpost length for buckling $r_{1_c1}$ using Eq. (23).

Additional variants of the two-link LSMS with self-offloading capability are illustrated in Fig. 6, which highlights alternative placements for spool 3 and cable *h3*. In this figure:

- **Blue** indicates the location of spool 2 and cable *h2*.
- **Purple** shows the position of spool 3 and cable *h3* as defined in the standard two-link configuration.
- **Orange** marks the spool 3 location as configured in the two-link self-offloading variant.
- **Red** represents the spool 3 and *h3* placement used in the LSMS-L35 LSMS configuration from a previous study.
- **Green** depicts the spool 3 and *h3* arrangement implemented in the LSMS-L1000 configuration, also based on prior work.

Mounting spool 3 lower on the LSMS, specifically along the *s1* link (as shown in both green and red in Fig. 6), offers the advantage of lowering the system's center of gravity. However, this design choice introduces tradeoffs, including increased cable length and additional loading on the kingpost, which collectively contribute to a higher overall system mass. Depending on mission requirements, these tradeoffs may be justified: particularly in scenarios where consolidating actuators near the base facilitates environmental shielding or simplifies maintenance and repair operations in the event of component failure.

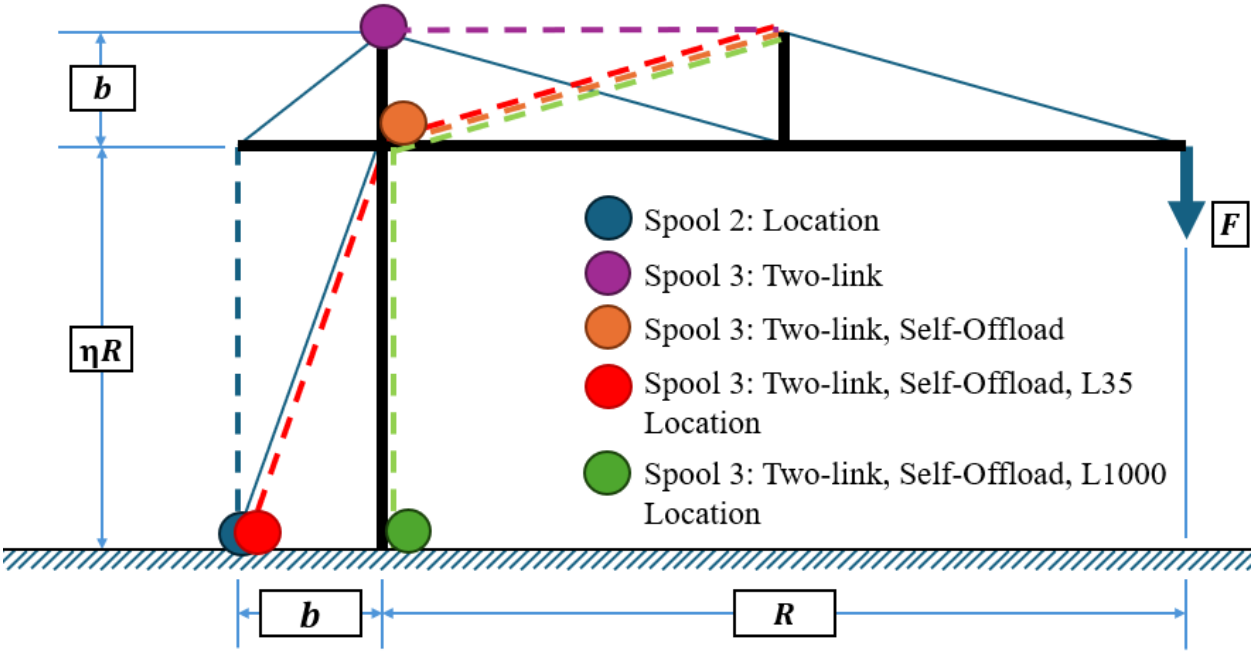



**Fig. 6 Possible spool location configurations for two-link LSMS.**

Moving spool 3 to the *s1* link has effects on member loads and therefore impact the sizing of the kingpost and the *s1* link. Sizing of the *s1* link is not highlighted in this paper as it is a member in bending and therefore requires different constraints in order to size. The updated kingpost (*c1*) force for the two-link with self-offloading LSMS-L1000 configuration (green spool 3 location) can be found using Eq. (51):

$$F_{c1} = F\left(1 + \frac{R + \sqrt{\left(\frac{R}{2}\right)^2 + b^2}}{b}\right) \tag{51}$$

The updated (*h3*) cable length for the two-link with self-offloading LSMS-L1000 configuration can be found using Eq. (52) below. As with all of the previous cable lengths, the exact amount of cable needed is highly dependent on the exact configuration and use case of the LSMS.

$$L_{h3} = (\eta \cdot R) + \sqrt{\left(\frac{R}{2}\right)^2 + b^2} + \left(2 \cdot D_{spool_h3} \cdot \pi\right) \tag{52}$$

The updated kingpost force and *h3* cable length for the two-link with self-offloading LSMS-L35 configuration are not highlighted in this paper due to the fact that they are highly dependent on other factors such as, *s1* to spreader length ratio, kingpost tilt, and loading of *t1* tension member.

## IV. LSMS Configuration Selection and Design Example

### A. LSMS Design Configuration Options

LSMS benefits from having multiple configurations allowing the system to be optimized for specific missions and use cases. Considering the offloading application at the onset of mission design is critical to properly select which, if any, LSMS configuration best suits the mission. For example, if the lander has multiple, small payloads that need to be transferred to the surface or a mobile agent with minimal manipulation and the offloading system mass must be minimized, then a one-link LSMS is a prime candidate. A one-link LSMS saves mass and complexity, while allowing offloading of multiple payloads if said payloads are shorter than the LSMS kingpost, as seen in Fig. 7. Fig. 7 also shows a simplified concept of a one-link LSMS picking up and placing a payload from a generic lander deck. Note the locations of the hoists are represented by circles.

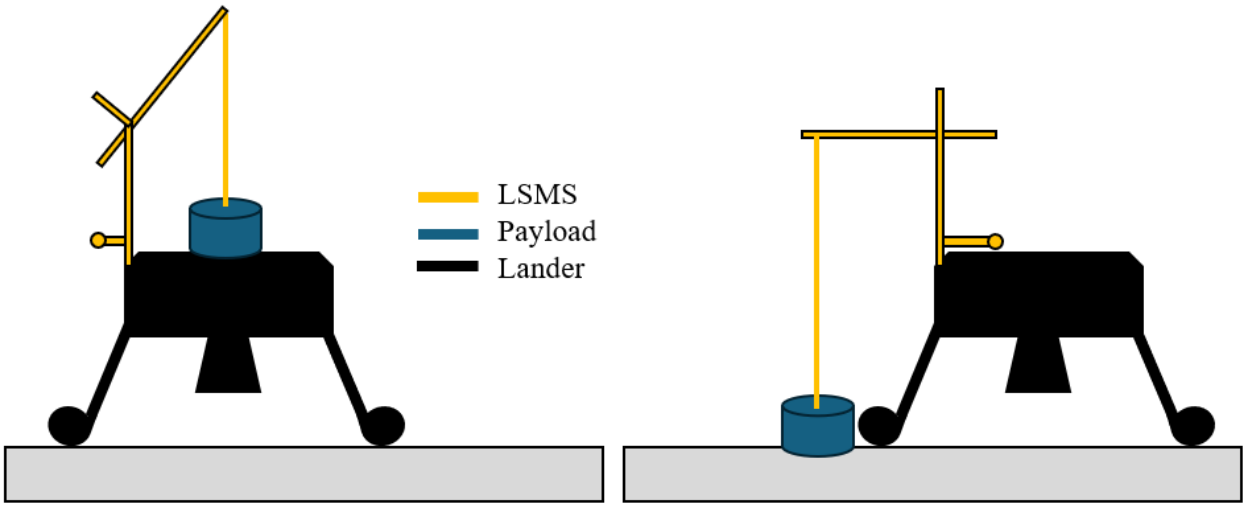



**Fig. 7 Example of one-link LSMS offloading lander.**

A one-link LSMS configuration is similar to a davit or single boom crane and is insufficient when a longer reach is required and the stowed LSMS configuration is not permitted to span the lander deck width. In such a case, a two-link LSMS configuration enables full reach of the lander deck and access to multiple payload delivery locations, as shown in Fig. 8.

A two-link configuration reduces the amount of cable required for any hoists needed at the wrist, as the wrist does not need as much height to arrive above a nearby payload unit. Compared to the two-link self-offloading configuration, the two-link also has a simpler design, lower mass and enables greater manipulability. The two-link variants of the LSMS also have the ability to lift payloads at the elbow (joint 3) with roughly twice the capacity of its design load at the tip.

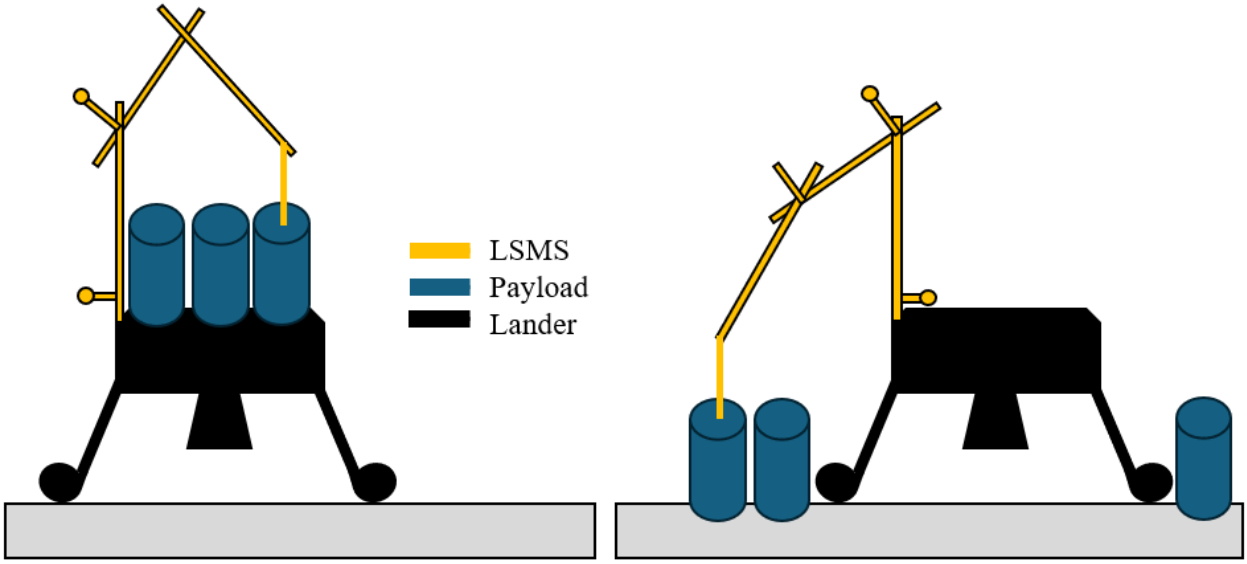



**Fig. 8 Example of two-link LSMS offloading lander.**

The two-link with self-offloading configuration is particularly advantageous if a) long or tall reach is required to unload a lander and b) the LSMS is offloaded from the lander to be used as a mobile or stationary surface asset. The two-link with self-offloading also benefits from being able to "touch its toes." This means the LSMS can pick up tall payloads packed near the kingpost. This added versatility largely comes from the addition of another link and degree of freedom allowing for additional end effector poses to be achieved. The center of gravity for a self-offloading configuration can also be lower to the ground due if the spool 3 locations on the *s1* link are selected due to the fact that the hoists, power supply, and electronics are all located at the base. For the same amount of reach, a two-link LSMS allows for more efficient, dense packing of the lander deck. The primary benefit of the two-link with self-offloading configuration remains the ability for the LSMS to offload itself from the lander onto the surface as it negates the need for a second dedicated offloader to move the LSMS from the lander deck to the surface as shown in Fig. 9.

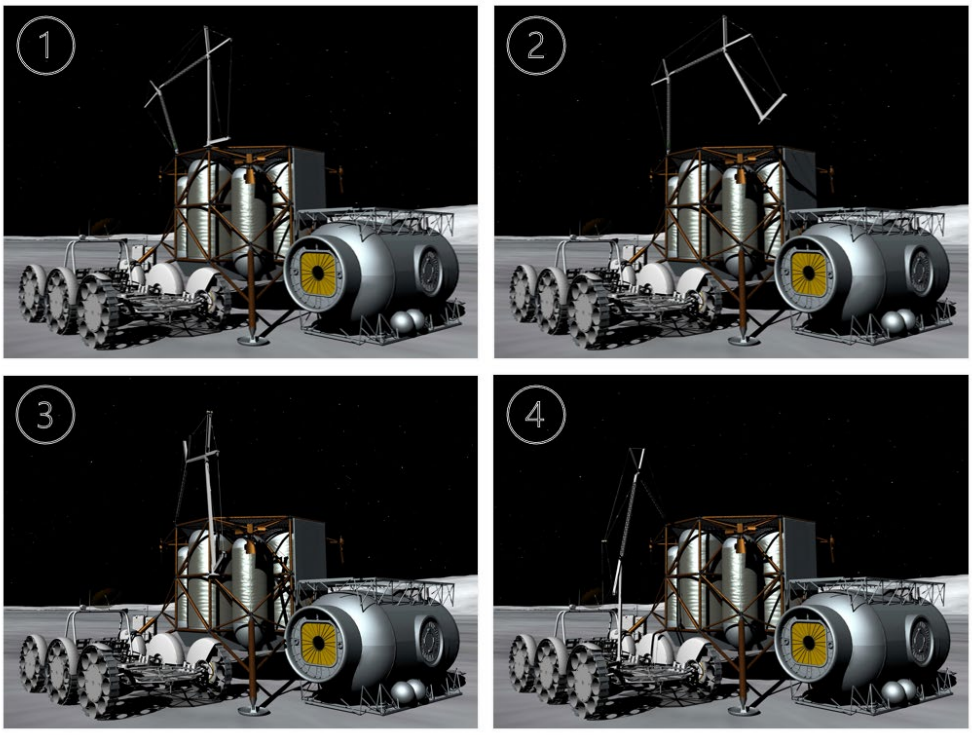



**Fig. 9 Conceptual example of a two-link LSMS self-offloading from a lander [9].**

## B. LSMS Design Sizing Example

Once the various LSMS configuration use cases are understood, selections for a reference mission can be made. As a design example, a lunar lander is to deliver a 40kWe fission surface power (FSP) reactor system to the lunar south pole that must be offloaded from the lander at the landing site to a mobile agent for transportation to its operational location. A 10 $kW_e$ FSP system has an estimated total mass of 3.5 metric tons, which is near the range of LSMS-L1000 mass capacity to offload (the capacity increases to 2000 kg at the elbow joint) [10]. For the design example, a 40 $kW_e$ FSP system is assumed to have a mass of 7 tons, rounded to a whole number based on the basic mass for such a system defined in Ref [11]. The FSP system consists of three components, a radiator module, the reactor, and a user interface for astronaut access. For the sake of the example, the components stacked together are assumed to create a wide cylinder shape measuring 5-m wide and 7-m tall that must be offloaded to the surface before the components are separated. The lander is assumed to be octagonal in shape and is 6-m wide from side-to-side. As there are no current offloading systems on the lunar surface, the lander must bring a dedicated offloading system. Mission architects would like to re-use the offloading system for future surface-based manipulation tasks. If one were to design an LSMS for such a design example, the two-link self-offloading configuration would be needed for two reasons. First, because the offloader is desired to be used later and elsewhere, meaning the LSMS would need to be offloaded from the lander after offloading the FSP reactor system. Second, as with the two-link configuration, due to space constraints on the lander deck, the LSMS should be stowed in a folded configuration along one side of the lander, seen to the left in Fig. 10, providing an upper limit to the length of each arm section that is shorter than the payload.

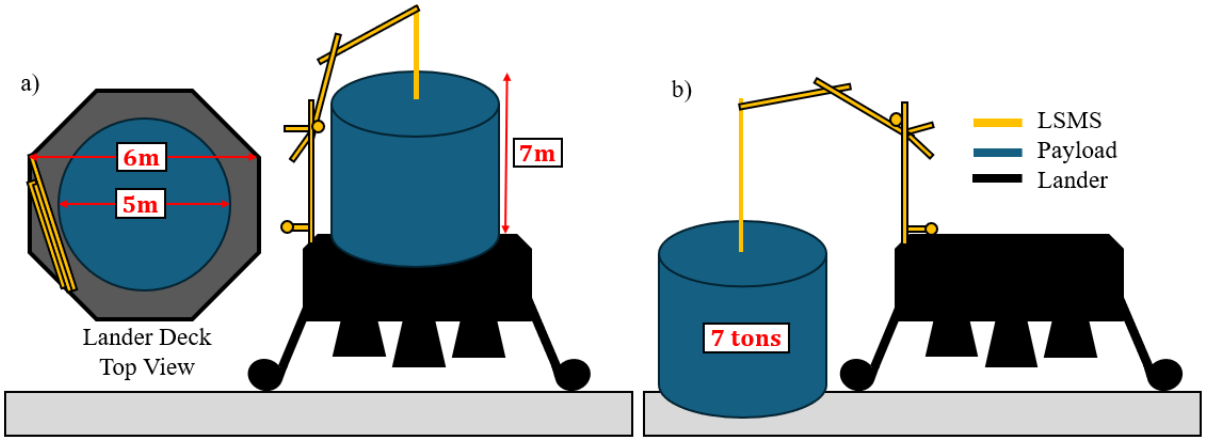



**Fig. 10 Example of two-link self-offloading LSMS offloading large FSP payload starting from a) stowed configuration on the left and b) delivering the payload to the surface.**

Therefore, a two-link, self-offloading LSMS is required for this application. It must be capable of lifting a payload of 7 tons with a reach of 6 m. The design specifies a kingpost whose length matches that of each arm. For this configuration, the initial design parameters include a tip force ($F$) of approximately 11,445 newtons, which results from the lunar gravitational acceleration acting on the 7,000-kilogram payload ($M_p$). The sweep radius ($R$) is set at 6 m, and the kingpost height factor ($\eta$) is set at 0.5 in order to produce a kingpost height equivalent to the arm and forearm lengths for more efficient packing. In this example, the spreaders are sized to keep the ratio of the spreader length ($b$) to the sweep radius ($R$) equivalent to $b/R$ used in the prior LSMS-L1000 configuration, which results in $b$ = 1.04 m for this example. Note that $b$ could be changed in a reasonable manner if needed to better meet mission requirements.

The design values and material properties used are detailed in Table 1. Member forces are calculated using statics principles under worst-case member loading condition of all links fully extended. These forces are resolved using the equations provided earlier in this paper, with results summarized in Table 2. Once the forces are known, member lengths are determined. For instance, the buckling length of the kingpost is calculated by combining its height with the spreader length, and this value is used to determine the cross-sectional area required to resist buckling. After establishing both the forces and lengths, the mass of each member is computed based on its material density and geometric properties. Rod density ($\rho_{rod}$) is used for members *t2a*, *t2b*, and *t2*; cable density ($\rho_c$) for *h2* and *h3*; and tube density ($\rho_{tube}$) for *c1*, *c2*, *s2a*, and *s2b*. The compression members are assumed to be constructed from aluminum and designed with a factor of safety of 4. Tension rods are assumed to be made of steel with a factor of safety of 2, while the cables are also assumed to be steel but require a higher factor of safety of 5.

**Table 1. Design example: User-defined material properties, factors of safety, and design parameters used.**

| Term | Value | Units | Term | Value | Units |
|---|---|---|---|---|---|
| $R$ | 6 | m | $\rho_c$ | 5,536 | kg/m$^3$ |
| $b$ | 1.04 | m | $\rho_{rod}$ | 1,661 | kg/m$^3$ |
| $t$ | 0.00635 | m | $\rho_{tube}$ | 2,768 | kg/m$^3$ |
| $F$ | 11,445 | N | $\eta$ | 0.5 | unitless |
| $M_p$ | 7,000 | kg | $k$ | 2 | unitless |
| $\sigma_c$ | 717,055 | kPa | $D_{overd}$ | 25 | unitless |
| $\sigma_{rod}$ | 413,685 | kPa | $FS_c$ | 5 | unitless |
| $\sigma_{al}$ | 310,264 | kPa | $FS_{rod}$ | 2 | unitless |
| $E_c$ | 68,947,600 | kPa | $FS_t$ | 4 | unitless |

**Table 2. Design example: Results for force, length, area, mass and associated equations used.**

| Member | Force Eq. | $F_n$ (N) | Length Eq. | $L_n$ (m) | Area Eq. | $A_n$ (m$^2$) | Mass Eq. | $M_n$ (kg) |
|---|---|---|---|---|---|---|---|---|
| **h2** | 29 | 66,029 | 11 | 6.8 | 18 | 0.000460 | 28 | 17.34 |
| **s2b** | 29 | 66,029 | 7 | 1.04 | 26 | 0.001862 | 28 | 5.36 |
| **c1** | 31 | 77,474 | 8 | 3 | 24 | 0.004862 | 28 | 40.38 |
| **t2b** | 32 | 93,379 | 12 | 1.47 | 15 | 0.000451 | 28 | 1.10 |
| **t3a** | 33 | 34,942 | 39 | 3.18 | 43 | 0.000169 | 28 | 0.89 |
| **t1** | 34 | 48,919 | 14 | 3.18 | 17 | 0.000118 | 28 | 0.62 |
| **c3** | 36 | 33,014 | 37 | 3 | 42 | 0.002999 | 28 | 24.90 |
| **s2a** | 45 | 88,919 | 7 | 1.04 | 27 | 0.002057 | 28 | 5.92 |
| **t2a** | 46 | 69,884 | 13 | 3.18 | 16 | 0.000338 | 28 | 1.78 |
| **h3** | 47 | 34,942 | 50 | 5.94 | 44 | 0.000244 | 28 | 8.01 |
| **s3a** | 48 | 22,890 | 38 | 1.04 | 41 | 0.001304 | 28 | 3.76 |
| **c2** | 49 | 99,043 | 6 | 3 | 25 | 0.004327 | 28 | 35.93 |
| | | | | | | | Total | 146 |

The total estimated mass of the members is 146 kg or approximately 2% of the payload mass (7 tons). Note that the structural mass estimate does not account for other major system components like joints, motors, gearboxes, and electronics.

## V. Concluding Remarks

The Lightweight Surface Manipulation System (LSMS) is a versatile, scalable architecture that is easily tailored for specific applications. A methodology is presented herein to rapidly size an instance of the LSMS for a desired application (lift capacity, reach). From mission-level requirements, such as reach and lifted mass, equations are provided to estimate structural member dimensions and loads. These closed-form equations are based on buckling and strength limits of the materials and cross sections calculated, which enable rapid estimation of candidate design details early in the design cycle, prior to detailed modeling or hardware commitments. Equations are outlined for three common configurations of the LSMS with square tube links: one-link, two-link, and two-link with self-offloading capability. Discussion of potential use cases for three common configurations are provided to aid selection of the best configuration for a given application. A design example is provided to illustrate application of the equations for the case of offloading a lunar fusion surface power reactor system (7 metric tons) with a two-link, self-offloading capable LSMS on the lunar surface. The equations provided and associated design philosophy are intended for early trade studies, where speed and traceability are paramount. The equations developed enable rapid exploration of feasible architecture capabilities to calculate resulting LSMS packaging mass and volume requirements for launch for

comparison with competing off-loading approaches such as ramps, davits, serial manipulators, traditional cranes and ejection systems. Ongoing development is expected to enhance the equations to include other subsystem masses beyond structural components such as actuators, while also taking into account the effect the mass of components contributes to member loads and therefore increased sizing. In addition, equations for advanced structural forms beyond square tubes such as truss links are being considered.

## Acknowledgments

The authors would like to thank Martin K. Mikulas and John T. Dorsey for their suggestions during the design of the devices discussed herein as well as guidance during development of the baseline equations presented to estimate the component sizes and overall mass of the devices.

## References

[1] Doggett, W. (Bill), Dorsey, J., Collins, T., King, B., Mikulas, M., and El-Genk, M. S., "A Versatile Lifting Device for Lunar Surface Payload Handling, Inspection & Regolith Transport Operations," *AIP Conference Proceedings*, Albuquerque, New Mexico, 2008, pp. 792–808. doi: 10.1063/1.2845045.

[2] SEIS, "The Instrument Deployment Arm (IDA)." URL: https://www.seis-insight.eu/en/public-2/the-insight-mission/the-ida-robotic-arm [retrieved: Apr. 25, 2025].

[3] Cline, J. E., Vaughan, M., Waltz, W., and Wong, I., "LANDO: Developing Autonomous Operations for Planetary Surfaces," *AIAA SCITECH 2022 Forum*, San Diego, CA & Online: American Institute of Aeronautics and Astronautics, Jan. 2022. doi: 10.2514/6.2022-0625.

[4] NASA, "NASA Lunar Surface Cargo." NASA. URL: https://www.nasa.gov/wp-content/uploads/2024/06/acr24-lunar-surface-cargo.pdf [retrieved: Apr. 25, 2025].

[5] Williams, D., "The Apollo Lunar Roving Vehicle." URL: https://nssdc.gsfc.nasa.gov/planetary/lunar/apollo_lrv.html [retrieved: Apr. 25, 2025].

[6] Gill, T. R., Gomez, J. D. J. Jr., Pittman, D., Lewis, M., Beaton, K., Chappell, S., and Kessler, P., "Lunar Surface Cargo Offloading Concepts," *51st International Conference on Environmental Systems (ICES 2022)*, Saint Paul, MN, July 10–14, 2022, Paper ICES-2022-38.

[7] Doggett, W. (Bill), King, B., Jones, T., Dorsey, J., and Mikulas, M., "Design and Field Test of a Mass Efficient Crane for Lunar Payload Handling and Inspection: The Lunar Surface Manipulation System," *AIAA SPACE 2008 Conference & Exposition*, San Diego, California, Sep. 2008. doi: 10.2514/6.2008-7635.

[8] Wong, I. M. and Cline, J. E., "LSMS – L35, Miniature Crane for Payload Off-loading and Manipulation: Development, and Application," *ASCEND 2022*, Las Vegas, Nevada, Oct. 2022. doi: 10.2514/6.2022-4237.

[9] Dorsey, J. T., Jones, T. C., Doggett, W. (Bill) R., Roithmayr, C. M., King, B. D., and Mikulas, M. M., "Developments to Increase the Performance, Operational Versatility and Automation of a Lunar Surface Manipulation System," *AIAA SPACE 2009 Conference & Exposition*, Pasadena, California, Sep. 2009. doi: 10.2514/6.2009-6795.

[10] Martin, J.R. and Cline, J.E., "The Potential of Offloading for Fission Surface Power Systems," *Nuclear Emerging Technologies for Space (NETS) 2025*, Huntsville, Alabama, May 5-7, 2025. DOI: 10.13182/NETS25-47317

[11] Oleson, S., Packard, T., Turnbull, E., Gibson, M., Rao, D., Barth, C., Wilson, S., Schmitz, P., Colozza, A., Klefman, B., Tian, L., and Mason, L., "A Deployable 40 kWe Lunar Fission Surface Power Concept*," Nuclear Emerging Technologies for Space (NETS) 2025*, Huntsville, AL, May 5-7, 2025. URL: https://ntrs.nasa.gov/api/citations/20220004670/downloads/40%20kW%20Deployable%20FSP%20Paper_FINAL.pdf [retrieved: Nov 25, 2025].